Combustion Characteristics of C_5 Alcohols and a Skeletal Mechanism for HCCI Combustion Simulation

Sungwoo Park[1], Suk Ho Chung[1], Tianfeng Lu[2], S. Mani Sarathy[1]*

[1]Clean Combustion Research Center, King Abdullah University of Science and Technology, Thuwal 23955-6900, Kingdom of Saudi Arabia

[2]Department of Mechanical Engineering, University of Connecticut, Storrs, Connecticut 06269-3139, United States

KEYWORDS

2-methylbutanol, iso-pentanol, ignition delay, intermediate temperature heat release, skeletal mechanism, HCCI engine combustion

ABSTRACT

C_5 alcohols are considered alternative fuels because they emit less greenhouse gases and fewer harmful pollutants. In this study, the combustion characteristics of 2-methylbutanol (2-methyl-1-butanol) and *iso*-pentanol (3-methyl-1-butanol) and their mixtures with primary reference fuels (PRFs) were studied using a detailed chemical kinetic model obtained from merging previously published mechanisms. Ignition delay times of the C_5 alcohol/air mixtures were compared with PRFs at 20 and 40 atm. Reaction path analyses were conducted at intermediate and high temperatures to identify the most influential reactions controlling ignition of C_5 alcohols. The direct relation graph with expert knowledge methodology was used to eliminate unimportant species and reactions in the detailed mechanism, and the resulting skeletal mechanism was tested at various homogeneous charge compression ignition (HCCI) engine combustion conditions. These simulations were used to investigate the heat release characteristics of the methyl-substituted C_5 alcohols, and the results show relatively strong reactions at intermediate temperatures prior to hot ignition. C_5 alcohol blending in PRF75 in HCCI combustion leads to a significant decrease of low temperature heat release (LTHR) and a delay the main combustion. The heat release features demonstrated by C_5 alcohols can be used to improve the design and operation of advanced engine technologies.

Introduction

Stringent emission regulations and health concerns related to the combustion of traditional fuels has elevated interest in alternative fuels and fuel additives. Oxygenated fuels have been considered alternative fuels or as fuel additives to fossil fuels because they emit less NO_x and particulates.[1] In addition, the production of oxygenated fuels from renewable sources can neutralize CO_2 emissions from combustion devices; however, before they are applied, their fundamental combustion characteristics need to be evaluated.[2] For example, although ethanol is a first-generation biofuel that has attractive characteristics as an alternative bio-based alcohol fuel extender for petroleum fuels, it also imparts disadvantages such as a high O/C ratio, high hygroscopicity, and low energy density, which can cause problems with fuel storage and blending in combustion engines. In contrast, higher alcohols have lower hygroscopicity and corrosivity, higher energy density, and can be readily blended with hydrocarbon fuels. Therefore, higher alcohol fuels, such as C_4 and C_5 alcohols, have been studied as next-generation biofuels, and extensive combustion chemistry studies on butanol isomers have been conducted over the last several years.[3-18]

The physical and chemical properties[1] of several alcohol fuels are presented in Table 1. The research octane number (RON) of 2-methylbutanol is unknown but could be estimated using the correlation between RON and shock tube (ST) ignition delay time under specific conditions (e.g., 835 K and 20 atm).[19] In general, the octane ratings of C_5 and larger alcohols are lower than those of C_1-C_3 alcohols; this higher propensity for ignition (increased cetane number) makes larger alcohols suitable for compression-ignition (CI) engine applications.[1]

Table 1. Physical and chemical properties of alcohol and gasoline.[1]

	ethanol	iso-butanol	iso-pentanol	2-methylbutanol[a]	Gasoline
Molecular weight	46.06	74.11	88.14	88.14	111.19
Oxygen content (wt%)	0.35	0.22	0.18	0.18	0
Lower heating value (MJ/L)	21.4	26.6	27.8	28.2	30-33
Boiling Point (°C)	78	108	130	129	27-225
RON	109	105	94	-	88-98
MON	90	90	84	-	80-88
Solubility in water at 25°C (wt%)	Miscible	8.1	2.7	3.8	Negligible

[a] values for 2-methylbutanol from Li et al.[20]

Attention to alcohol combustion research on a C_5 family of alcohols, including *n*-pentanol[21-25], *iso*-pentanol (3-methyl-1-butanol, 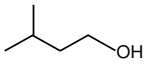)[26-30], and 2-methylbutanol (2-methyl-1-butanol, 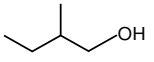)[31-34] has increased in recent years because longer-chain alcohols are better suited for combustion engines. However, there have been limited studies on C_5 alcohol combustion. Tang et al.[24] measured the high-temperature ignition delay times of C_5 alcohols (*n*-pentanol, *iso*-pentanol, and 2-methylbutanol) in shock tubes with varying equivalence ratios at temperatures above 1100 K and pressures of 1 and 2.6 atm. Their experimental results showed that the ignition delay times and global activation energy decreased in the order of *iso*-pentanol to 2-methylbutanol to *n*-pentanol. The CNRS Orleans group measured the concentrations of reactants, intermediate species, and products of *iso*-pentanol[26] and 2-methylbutanol[31] in a jet-stirred reactor at 10 atm and simulated their experiments using detailed chemical kinetic mechanisms. In 2012, Zhao et al.[22] calculated pressure- and temperature-dependent rate constants for the thermal decomposition of pentanol isomers. In the same year, Welz and co-workers[28] studied the low-temperature oxidation pathways of *iso*-pentanol using photoionization mass spectrometry to emphasize the importance of the formation of *iso*-pentanal (3-methylbutanal) and enol species. More recently, Lucassen and co-workers investigated the

combustion chemistry of 2-methylbutanol[33] and *iso*-pentanol[30] in low-pressure premixed flames using flame-sampling molecular-beam mass spectrometry along with detailed chemical kinetic models. In 2013, Li and co-workers[20,25] measured laminar-burning velocities of C_5 alcohol isomers at elevated temperatures and pressures using a spherically propagating flame. And earlier this year, Zhang et al.[32] measured pyrolysis species of 2-methylbutanol in a flow reactor using synchrotron vacuum ultraviolet photoionization mass spectrometry at low and atmospheric pressures. Their results showed that the decomposition of 2-methylbutanol is similar to that of *iso*-butanol rather than that of *n*-butanol. Previously, Tsujimura et al.[27] proposed a chemical kinetic model for *iso*-pentanol, including comprehensive reaction pathways at low, intermediate, and high temperatures, and validated it against ignition delay times. Meanwhile, Sarathy and co-workers[29] provided a wide range of experimental data for the oxidation of *iso*-pentanol and proposed a detailed chemical kinetic model. Most recently, Park et al.[34] proposed a chemical kinetic model for 2-methylbutanol and compared it against existing and new experimental data on its combustion.

Longer-chain alcohols could significantly increase the biofuel content in blended fuels due to their higher energy content, better engine compatibility, and lower water solubility. Campos-Fernández et al.[35] studied the short-term performance of a direct-injection diesel engine fueled with different *n*-pentanol/diesel fuel blends and found a slight engine power loss and an increase in brake thermal efficiency when the engine was fueled with higher alcohol blends. In 2000, Gautam and Martin[36] investigated the combustion characteristics of alcohol/gasoline blends in a single-cylinder engine and their results showed that higher-alcohol/gasoline blends have a greater resistance to knock than neat gasoline. Ten years later, Yang and co-workers[37] studied the fundamental characteristics of *iso*-pentanol as a fuel for homogeneous charge

compression ignition (HCCI) engines. They found that *iso*-pentanol displays intermediate temperature heat release (ITHR) characteristics, which is important for optimal engine operation. HCCI engines combine the advantages of a spark ignition (SI) engine with a CI engine, but they struggled to control the ignition delay time and the rate of combustion.

The purpose of this study is to investigate the ignition and heat release characteristics of methyl-substituted pentanol isomers, 2-methylbutanol and *iso*-pentanol, to improve our understanding of their combustion with analyses using a detailed chemical kinetic model. We also present a new skeletal mechanism suitable for HCCI combustion simulations and test the model against various HCCI engine conditions to help explain the combustion properties of C_5 alcohols in an HCCI engine for a wide range of conditions including intake pressure, intake temperature, and engine speed.

Chemical kinetic model

All simulations were conducted in CHEMKIN PRO 15112[38] using the appropriate reactor modules. The detailed chemical kinetic model used in this study results from the merging of previously published mechanisms. The AramcoMech 1.3[39] for the oxidation of small hydrocarbon was utilized as the base mechanism, which has been widely validated for C_1-C_2 species for improved prediction of ignition delay times, flame speeds, and flame speciation. The 2-methylbutanol[34] and iso-pentanol[29] sub-schemes were included for low- and high-temperature chemistry of C_5 alcohols, which have been previously validated against various experimental data sets such as ignition delay times, laminar burning velocity, and species mole fraction in jet-stirred reactor (JSR). The LLNL (Lawrence Livermore National Laboratory) Gasoline Surrogate sub-scheme[40] was also added to allow computations of C_5 alcohols mixed with primary reference

fuels (PRFs). The resulting detailed mechanism used in this study involved 1482 species and 6573 reaction steps. The detailed and skeletal mechanisms and thermodynamic properties are available as supplementary material.

Results and discussion

Autoignition delay times

Ignition delay times for a) stoichiometric and b) fuel-lean (ϕ = 0.5) 2-methylbutanol and *iso*-pentanol in air were simulated using the adiabatic constant volume homogenous reactor model in CHEMKIN PRO[38], and the results were compared with experimental data[27,34] at 20 atm, as shown in Figure 1. The model was also tested against ignition delay times measured in the rapid compression machine (RCM) by running homogeneous variable volume history simulations accounting for the compression stroke and post-compression expansion/heat loss in the experiments. In this study, the onset of ignition for constant volume simulation is the time corresponding to the maximum rate of temperature rise (max dT/dt), which corresponds to the maximum pressure rise rate (max dP/dt). The ignition delay time in the RCM is defined as the difference in time between the end of compression and the maximum of the time derivative of the pressure. The ignition data for *iso*-pentanol/air mixtures were measured using a ST at NUI (National University of Ireland) Galway and an RCM at the University of Connecticut[27], and the data for 2-methylbutanol/air mixtures were obtained using a high-pressure shock tube (HPST) at KAUST[34]. Overall, the proposed model for C_5 alcohols well predicts the ST and RCM experimental data within a factor of 2. Figure 1 also presents the ignition data for PRF84[41] (a mixture of 84% *iso*-octane and 16% *n*-heptane in volume fraction). Experimental and computational results indicate that the ignition delay times of 2-methylbutanol/air mixtures are

similar to those of *iso*-pentanol/air mixtures at intermediate temperatures (950-1050 K), but, at higher temperatures (T > 1050 K), ignition delay times and overall activation energy of 2-methylbutanol are lower than those for *iso*-pentanol. In contrast, the simulated ignition times of 2-methylbutanol are longer than those of *iso*-pentanol at the lowest temperatures. The ignition behavior of both fuels in the high-temperature region is consistent with shock tube ignition data acquired at 1 and 2.6 atm by Tang et al.[24] Figure 1 also shows that the ignition times of C_5 alcohols are slightly faster than for PRF84 in the intermediate-temperature region (950-1050 K). However, pronounced negative temperature coefficient (NTC) behavior is observed for PRF84, and the ignition delay times of *iso*-pentanol become slower than PRF84 near the NTC transition region, where low-temperature reactivity of PRF84 increases. The simulated ignition times of C_5 alcohols also show decreased reactivity under low-temperature conditions.

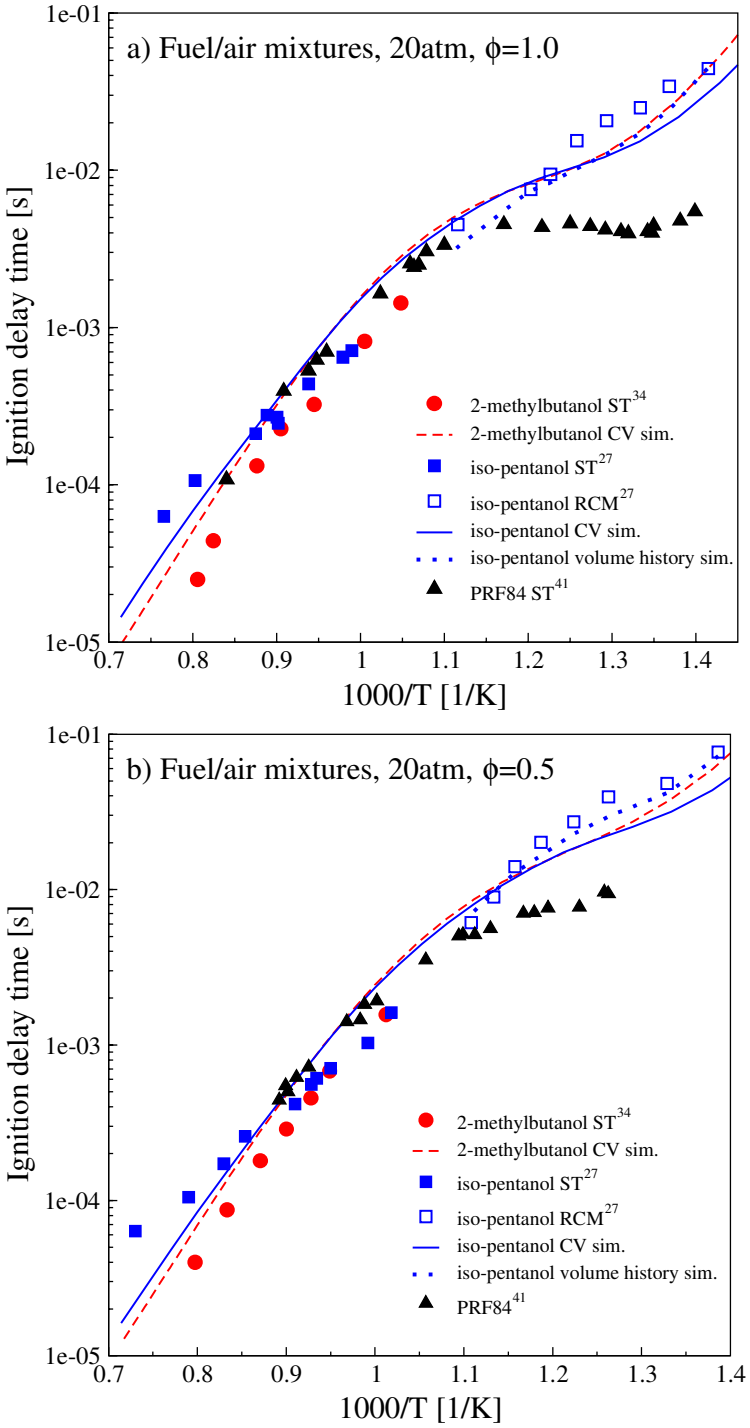

Figure 1. Ignition delay times for 2-methylbutanol[34] and iso-pentanol[27] compared with simulations at 20 atm. Experimental data for PRF84[41] are also presented.

Ignition delay times for 2-methylbutanol and *iso*-pentanol in air were also compared at 40 atm using the HPST at KAUST[34], and ignition data for *iso*-pentanol/air mixtures were measured in a ST at the Rensselaer Polytechnic Institute[29]. Figure 2 displays the experimental data at 40 atm for stoichiometric fuel/air mixtures with *n*-heptane[42], PRF84[41], and *iso*-octane[42]. We observed a similar trend at 40 atm as was observed at 20 atm. In the intermediate temperature region (800-1000 K), the ignition data of 2-methylbutanol/air mixtures are very close to *iso*-pentanol/air ignition data, but at high temperatures, ignition delay times of 2-methylbutanol are shorter than for *iso*-pentanol. (i.e., ignition delay times and overall activation energy of 2-methylbutanol are lower than *iso*-pentanol). Between intermediate- and high-temperatures, the ignition delay times of C_5 alcohols are also slightly faster than for *iso*-octane and PRF84. However, ignition delay times for both C_5 alcohols becomes slower than for *n*-heptane, PRF84, or *iso*-octane at the lowest temperatures due to a lack of low-temperature reactivity of C_5 alcohols.

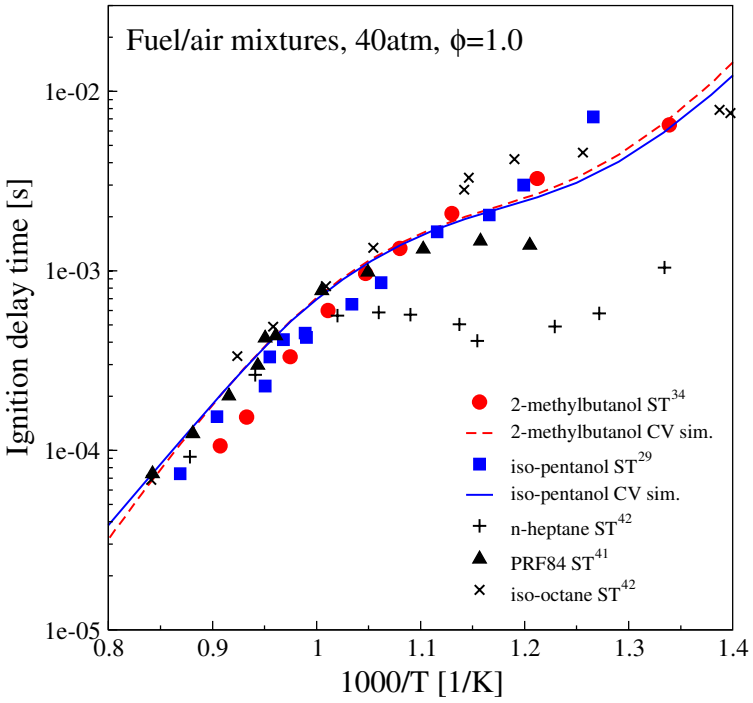

Figure 2. Ignition delay times for 2-methylbutanol[34] and iso-pentanol[29] compared with simulations at 40 atm. Experimental data for n-heptane[42], PRF84[41], and iso-octane[42] are also presented.

To highlight the most influential reactions controlling the ignition of both C_5 alcohol/air mixtures, reaction path analyses for stoichiometric and fuel lean (ϕ=0.5) mixtures were conducted at 950 and 1350 K under 20 atm using the detailed chemical kinetic model. Figure 3 displays the dominant reaction pathways for the consumption of a) 2-methylbutanol and b) *iso*-pentanol; italicized and bold texts refer to intermediate- (950K) and high-temperature (1350K) conditions, respectively. The reaction paths were obtained from the rate of production analysis in CHEMKIN PRO[38] at a time corresponding to 20% of the fuel consumed. Fuels are mainly consumed by H-atom abstraction reactions in favor of the α-site at 950 K because of its low C-H bond dissociation energy. Approximately 50% of fuels are consumed by the H-atom abstraction at the α-site to produce α-hydroxypentyl radicals, which mainly react with molecular oxygen to produce C_5 aldehyde species and HO_2 (2-methylbutanal from 2-methylbutanol and *iso*-pentanal from *iso*-pentanol). These reactions are low-temperature chain terminating pathways that inhibit low-temperature ignition of alcohols.[43] The other fuel radicals are confronted with competition between β-scission decomposition reactions and O_2 addition reactions to radical sites to form hydroxypentyl peroxy (ROO) radicals (gray pathways in Figure 3). These ROO radicals mainly undergo isomerization to form hydroxypentyl hydroperoxide (QOOH), the conventional low-temperature chain-branching reaction. Therefore, fuel ignition is largely dependent on the formation of 2-methylbutanal and *iso*-pentanal as well as low-temperature chemistry at 950 K. H-atom abstraction reactions are still the dominant fuel consumption pathways at 1350 K favoring the α-site. In addition, the unimolecular fuel decomposition reactions become important under high-temperature conditions. Approximately 16% of 2-methylbutanol is decomposed to

form 2-butyl and hydroxymethyl radicals, and the formation of methyl and ɣ-hydroxybutyl radicals accounts for 6% of *iso*-pentanol consumption. Subsequently, β-scission reactions of fuel radicals lead to the formation of smaller radicals and unsaturated species (e.g., alkenes, enols, and/or aldehydes) in favor of C-C or C-O bond cleavage. Ethylene (C_2H_4) and butene isomers (C_4H_8, 1-butene, 2-butene) are major intermediate species of 2-methylbutanol, while propene (C_3H_6) and *iso*-butene (iC_4H_8) are major intermediate species of *iso*-pentanol. Fuel consumption pathways are insensitive to equivalence ratio, but O_2 addition reactions become more important at 950K for lean mixtures due to the higher O_2 mole fraction.

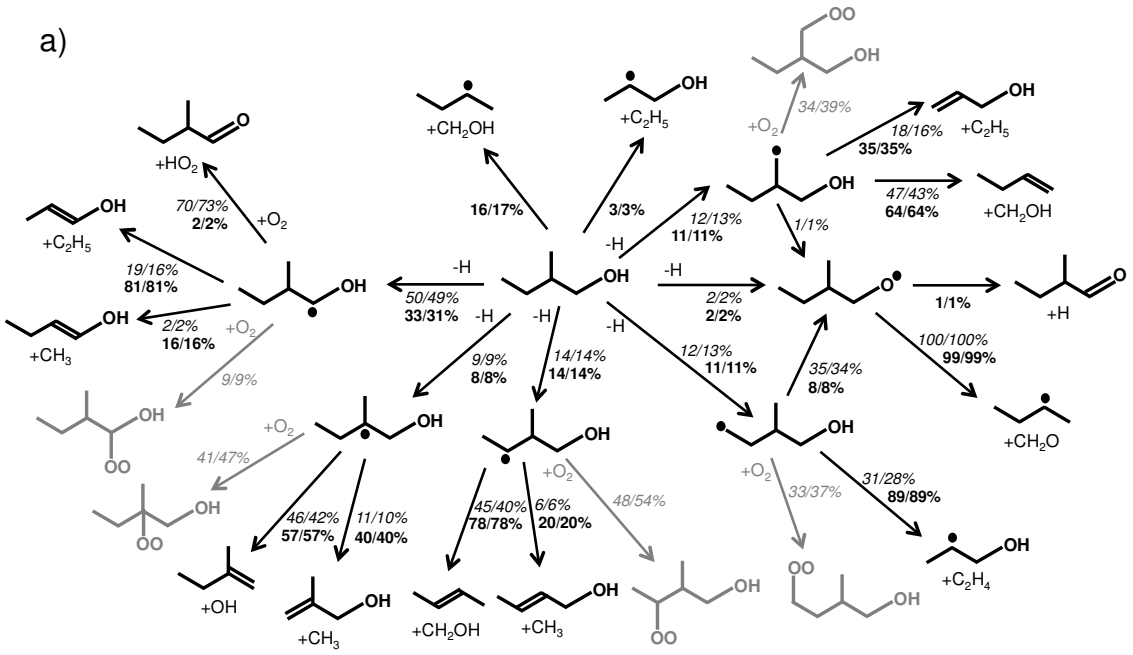

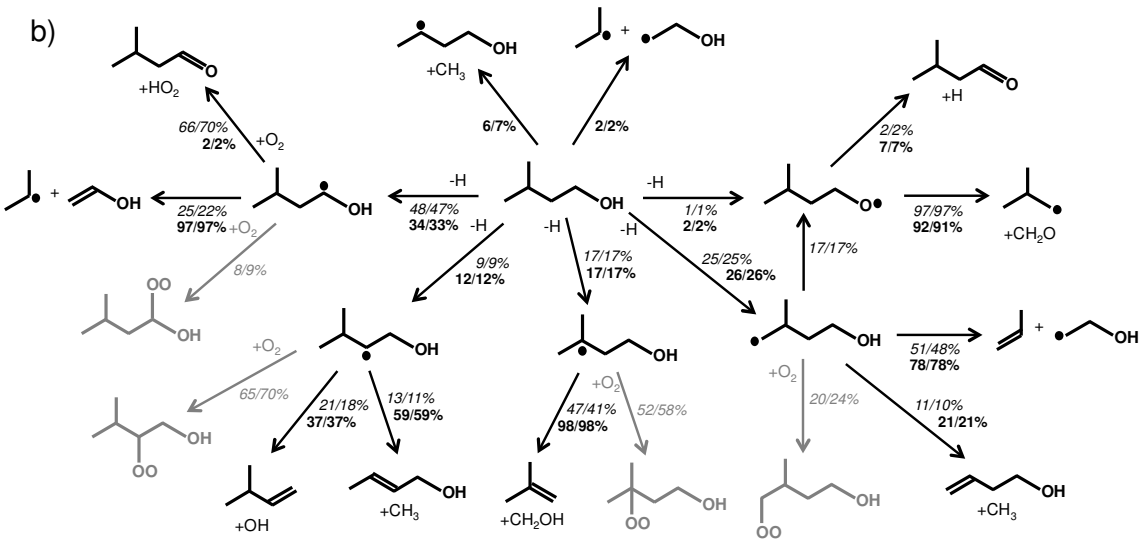

Figure 3. Reaction path analysis for a) 2-methylbutanol and b) iso-pentanol at 950 K (italics) and 1350 K (bold) under 20 atm (ϕ = 1.0/0.5). The reaction fluxes correspond to the time when 20% of the fuel was consumed.

Figure 4 presents the comparison of temperature and major intermediate species identified in the fuel consumption path analyses. C_5 aldehyde species (2-methylbutanal and *iso*-pentanal) appear as major intermediate species in the early stage of ignition at 950 K, while ethylene for 2-methylbutanol and propene for *iso*-pentanol increase rapidly before ignition occurs. However, under high-temperature conditions (1350 K), ethylene and propene remain the dominant intermediate species. As expected from the reaction path analyses, ethylene is a major intermediate species for 2-methylbutanol/air mixtures, while propene is dominant during the ignition of *iso*-pentanol/air mixtures. Ethylene is more reactive than propene, and the different reactivity of C_5 alcohols at high-temperature conditions can be explained by this different formation of major intermediate species. Although the present detailed mechanism well reproduces the experimental ignition data qualitatively and quantitatively, further fundamental chemical kinetic studies for larger alcohols are needed to determine more accurate reaction pathways and rate constants.

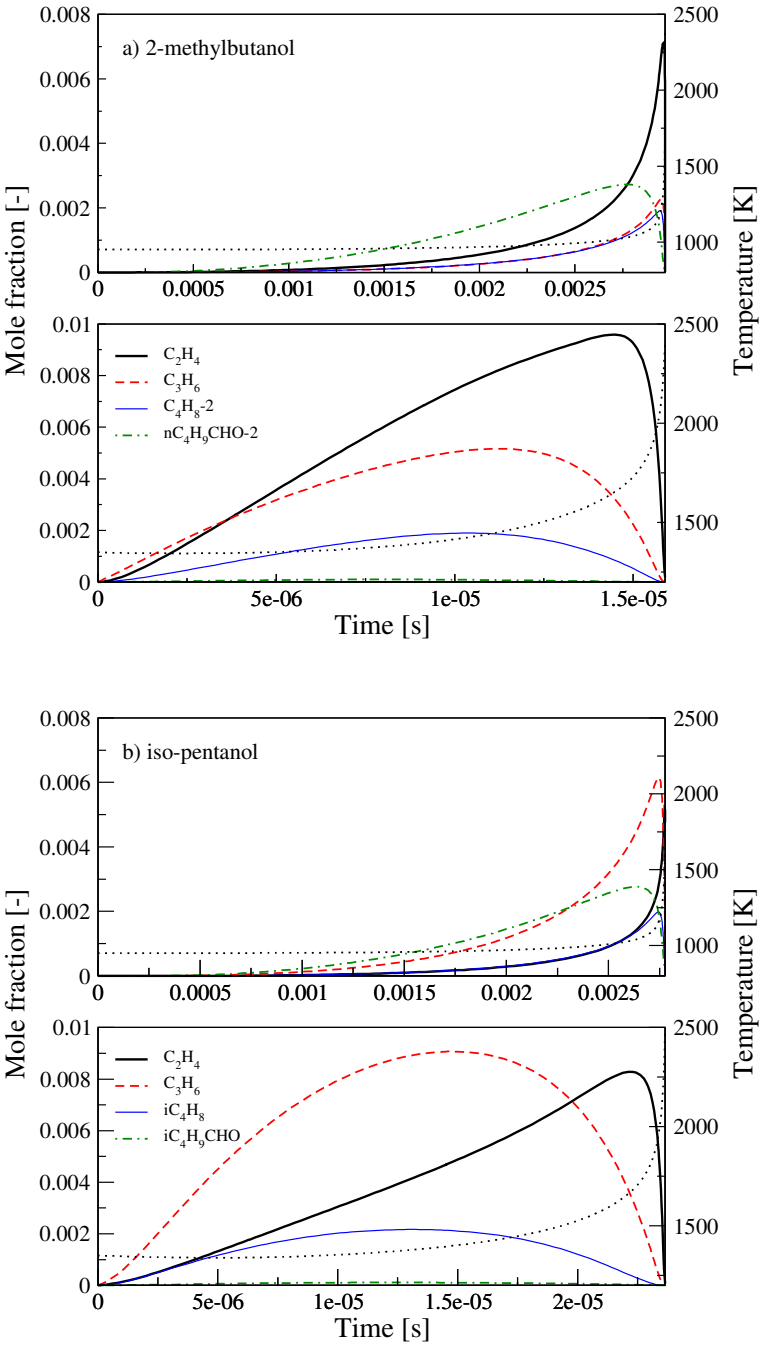

Figure 4. Predicted major intermediate species (ethylene, propene, 2-butene, iso-butene, 2-methylbutanal, and iso-pentanal) and temperature profiles for a) 2-methylbutanol and b) iso-pentanol at 20 atm, ϕ = 1.0, 950K (top) and 1350 K (bottom).

Heat release in an HCCI engine

The homogeneous charge compression ignition (HCCI) has been studied extensively as an alternative internal combustion (IC) engine process to the conventional premixed SI engine and non-premixed CI engine. Yang and co-workers experimentally studied the fundamental characteristics of *iso*-pentanol as a fuel for HCCI engines[37], while Tsujimura et al.[44] simulated the results using a detailed chemical kinetic model. Their results indicated that *iso*-pentanol shows characteristics of intermediate temperature heat release (ITHR). HCCI engine simulations were conducted using a detailed chemical kinetic model to explain the heat release characteristics of C_5 alcohols. Simulations were performed at an intake pressure (P_{in}) of 150 kPa, a compression ratio (CR) of 14, an engine speed of 1200 RPM, an equivalence ratio of 0.3, and varied intake temperatures (T_{in}) to maintain CA50 = 368CAD using a single-zone homogeneous adiabatic combustion model in CHEMKIN PRO[38]. The simulation results of *iso*-octane and PRF75 are also displayed using the present detailed mechanism. Figure 5 shows the comparison of accumulated heat release and heat release rates of C_5 alcohols (normalized by total heat release) with those of *iso*-octane and PRF75 at an early stage of heat release. C_5 alcohols show relatively strong heat release prior to hot ignition. Figure 5 also indicates C_5 alcohols are more reactive than *iso*-octane, and these results are consistent with previous *iso*-pentanol studies on HCCI combustion.[37,44] The required intake temperature of reactive fuels is lower than that for less reactive fuels at constant desired combustion phasing.

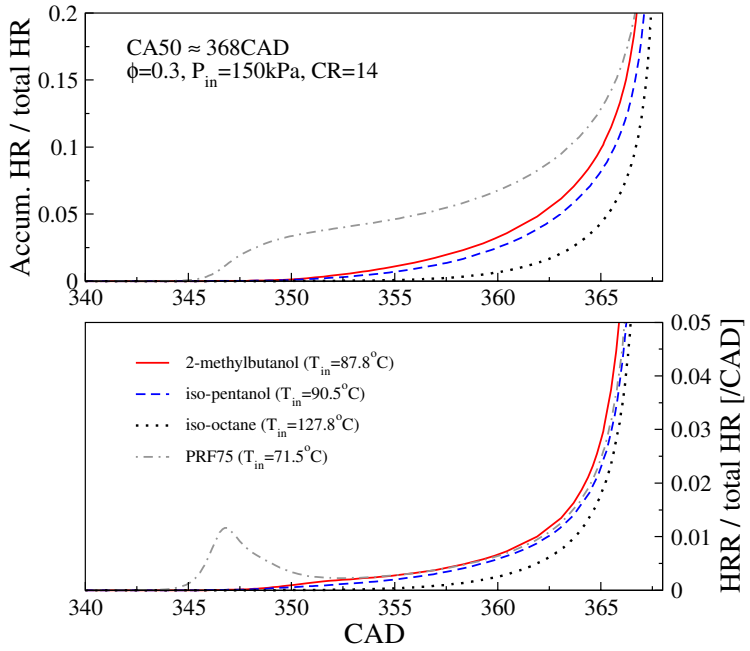

Figure 5. Comparison of accumulated heat release and heat release rate of 2-methylbutanol and iso-pentanol with those of iso-octane and PRF75. (CA50≈368CAD, ϕ =0.3, P_{in}=150 kPa, and CR=14).

To quantify the boundaries of ITHR, the heat release rate (HRR) derivative-based method[45] was employed to identify the sudden change in HRR. The start of the ITHR is defined at the point where the second derivative of the heat release is equal to zero with an upper limit set at 0.004 (1/deg^2). Figure 6 presents the comparison of heat release profiles for C_5 alcohols with iso-octane and PRF75 and the concentration profiles for formaldehyde (CH_2O). During the ITHR period, formaldehyde is present at a significant concentration but is consumed quickly during high-temperature heat release.[45] The results show that PRF75 exhibits clear low-temperature heat release, while both 2-methylbutanol and *iso*-pentanol display considerably more prominent ITHR behavior than *iso*-octane under the given conditions. The rate of temperature rise prior to hot ignition is important for maintaining the stability of HCCI

combustion, wherein retarding combustion phasing by increasing ITHR allows for a more moderate rate of pressure increase while avoiding misfire.[46]

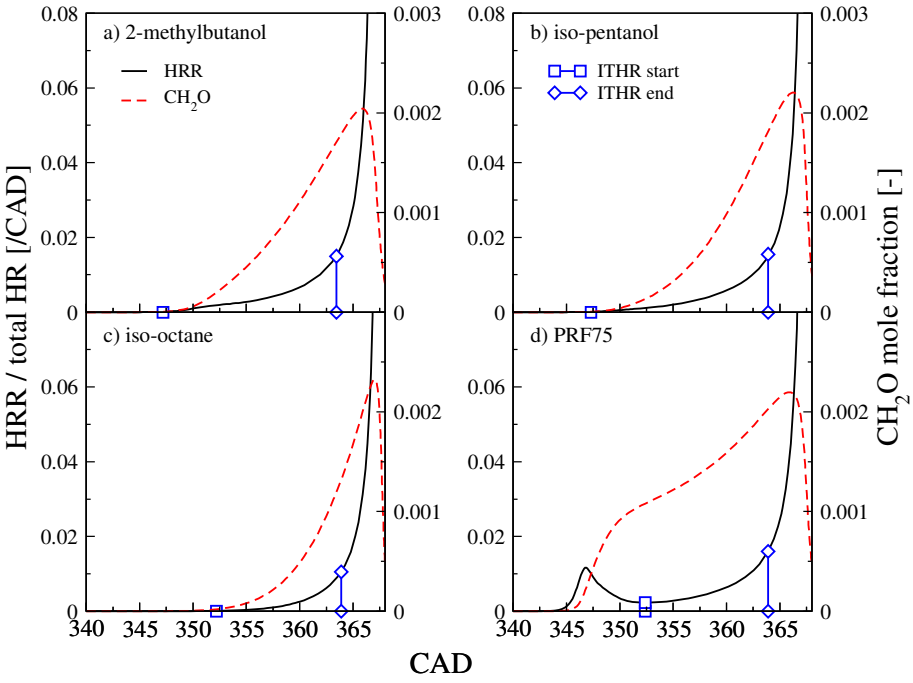

Figure 6. Comparison of ITHR boundaries of 2-methylbutanol and iso-pentanol with those of iso-octane and PRF75. (CA50≈368CAD, ϕ =0.3, P_{in}=150 kPa, and CR=14). Concentration profiles of formaldehyde are also presented.

Figure 7 presents the dominant reactions of C_5 alcohols contributing to the heat release rate at 8^o before CA50 to provide insight into the ITHR (930~950K). To simplify the analysis, H-atom abstraction reactions by OH radicals and fuel radical reactions with O_2 were grouped together to calculate the sum of heat release. The results indicate that the most important reactions contributing to the rate of heat release are the reactions between fuel radicals and molecular oxygen (R+O_2 reactions), as well as H-atom abstraction by OH radicals (fuel+OH=R+H_2O reactions). In addition, hydrogen peroxide formation paths by the recombination of HO_2 radicals via H+O_2 reaction are also important for heat release during

ITHR, but the rapid decomposition reaction of H_2O_2 to OH radicals is endothermic to partially reduce the heat release from the above reactions at relatively high temperatures (930~950K).

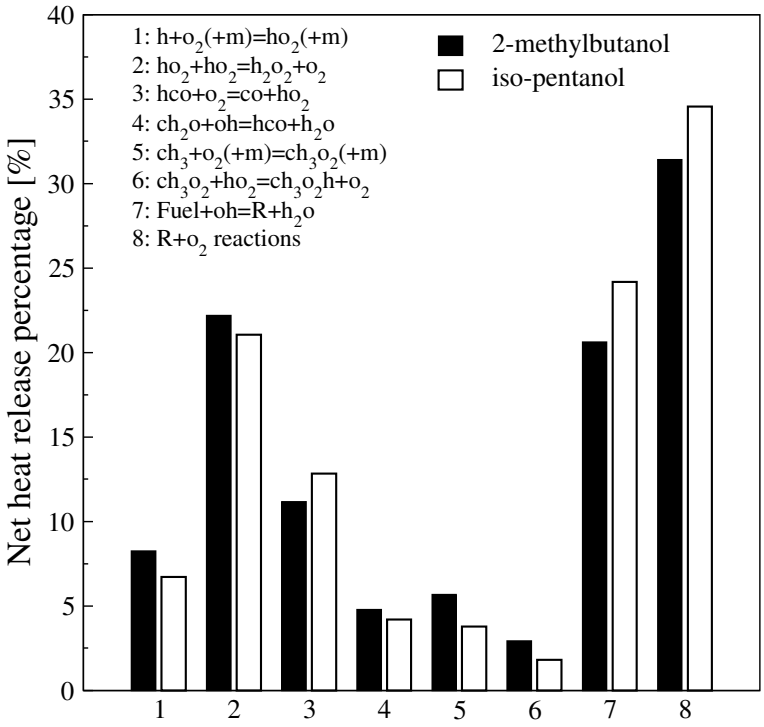

Figure 7. Net heat release by elementary reactions of C_5 alcohols as a percentage of ITHR 8^o before CA50. (CA50≈368CAD, ϕ =0.3, P_{in}=150 kPa, and CR=14).

Mechanism reduction with DRGX

The direct relation graph (DRG) with expert knowledge (DRGX) method[47,48] was used to develop a skeletal mechanism for HCCI engine combustion simulations. The DRG[49] method is based on the observation that weakly coupled species during combustion process can be eliminated. The first step in DRG is to quantify species coupling by the pair-wise error, r_{AB}, induced to a species A by the elimination of another species B for a given temperature and species concentrations. Figure 8 shows a typical species relations in a DRG. The arrow shows

the direction of dependence with the line weight indicating the relative importance. It is seen that A depends on B, but B does not depends on A. Moreover, species B and D are strongly coupled to form the dependent set {B,D} of A and have to be kept for correct prediction of A. However, species C, E and F can be eliminated because they are not required either A or any dependent set {B,D} of A.

$$r_{AB} \equiv \frac{\max_i |\nu_{Ai}\omega_i\delta_{Bi}|}{\max_i |\nu_{Ai}\omega_i|} \quad \delta_{Bi} = \begin{cases} 1, \text{if the } i\text{th reaction involves } B \\ 0, \text{otherwise} \end{cases}$$

ω_i: net reaction rate of the ith reaction
ν_{Ai}: stoichiometric coefficient of species A in the ith reaction.

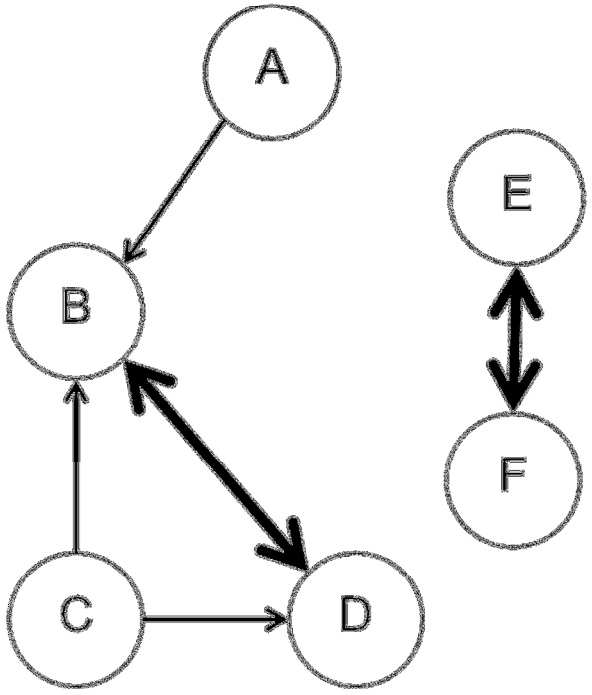

Figure 8. Typical species relation in a direct relation graph.

Compared to the original DRG, DRGX allows for species-specific error control employing a revised depth-first search (RDFS).[50] Species-specific error tolerances can be used for selected species with small uncertainties for associated reactions. Any species B having larger r_{AB} than specified error tolerance will be retained in the skeletal mechanism, while other

species are treated using a default error tolerance. Such expert-specified species-specific information renders it possible to develop a highly accurate skeletal mechanism for heat release or species concentrations of interest.

Here, we performed a DRGX on sampled data from auto-ignition and a perfectly stirred reactor (PSR) model in a parameter range relevant to our HCCI combustion for C_5 alcohols and PRF75. The reduction covers pressures of 1, 20, and 40 atm, equivalence ratios between 0.3 and 1.0, initial temperatures for ignition from 650 to 1400 K, and an inlet temperature of 400 K for PSR. By specifying an error tolerance of 0.05 for temperature, 0.2 for H and OH radicals, and a default error tolerance of 0.45, the resulting skeletal mechanism consists of 631 species and 3233 reaction steps from the detailed mechanism by assigning 3 independent fuels (2-methylbutanol, iso-pentanol, and PRF75) as input parameters. The comparisons of laminar flame speed and jet-stirred reactor (JSR) species profiles using the skeletal mechanism are provided in the Supplementary material.

Skeletal mechanism for HCCI simulation

Before using the skeletal mechanism under HCCI engine combustion conditions, the skeletal mechanism was compared with the detailed mechanism. Figure 9 shows the ignition delay times of a) 2-methylbutanol, b) *iso*-pentanol, and c) PRF75 in air at 20 and 40 atm. Simulations were conducted using the adiabatic constant volume homogenous reactor model in CHEMKIN PRO[38]. The skeletal mechanism is in excellent agreement with the detailed mechanism covering pressures of 20 and 40 atm at equivalence ratios of 0.3, 0.5, and 1.0, which corresponds to HCCI engine simulation conditions.

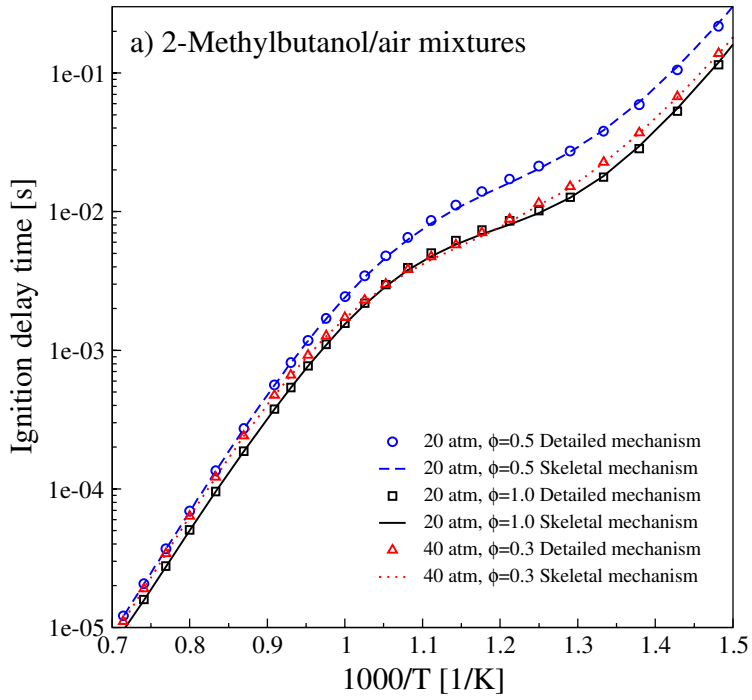
a) 2-Methylbutanol/air mixtures
Ignition delay time [s]
1000/T [1/K]
1e-01
1e-02
1e-03
1e-04
1e-05
0.7
0.8
0.9
1
1.1
1.2
1.3
1.4
1.5
20 atm, ϕ=0.5 Detailed mechanism
20 atm, ϕ=0.5 Skeletal mechanism
20 atm, ϕ=1.0 Detailed mechanism
20 atm, ϕ=1.0 Skeletal mechanism
40 atm, ϕ=0.3 Detailed mechanism
40 atm, ϕ=0.3 Skeletal mechanism

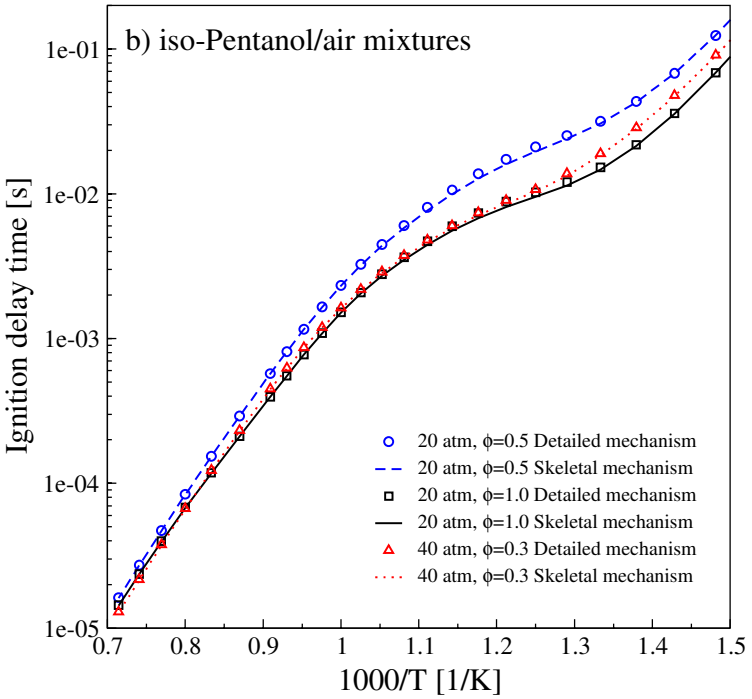
b) iso-Pentanol/air mixtures
Ignition delay time [s]
1000/T [1/K]
1e-01
1e-02
1e-03
1e-04
1e-05
0.7
0.8
0.9
1
1.1
1.2
1.3
1.4
1.5
20 atm, ϕ=0.5 Detailed mechanism
20 atm, ϕ=0.5 Skeletal mechanism
20 atm, ϕ=1.0 Detailed mechanism
20 atm, ϕ=1.0 Skeletal mechanism
40 atm, ϕ=0.3 Detailed mechanism
40 atm, ϕ=0.3 Skeletal mechanism

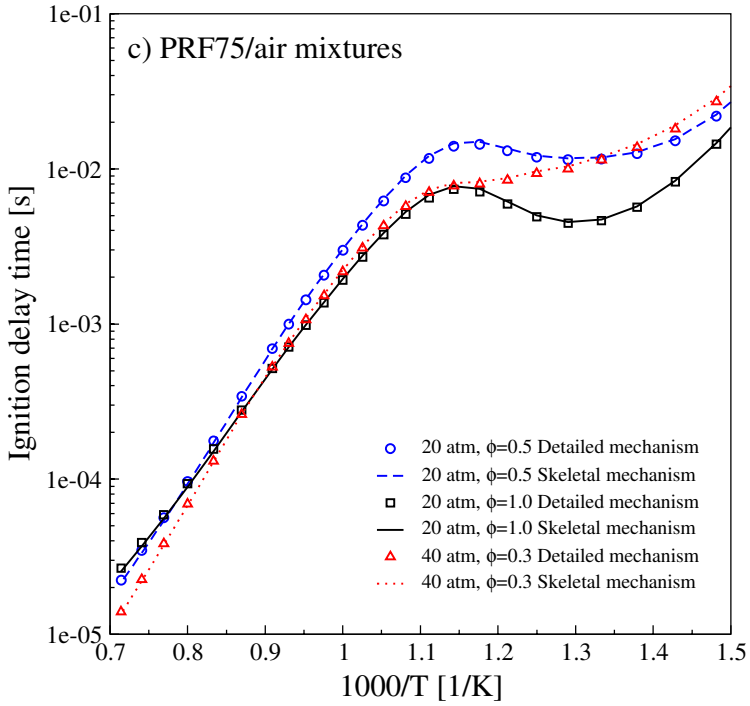

Figure 9. Comparison between detailed (dashed lines) and skeletal (solid lines) mechanisms for ignition delay times of a) 2-methylbutanol, b) iso-pentanol, and c) PRF75.

HCCI engine simulations were performed at the same conditions of the above mentioned HCCI simulation (intake pressure (P_{in}) : 150 kPa, CR : 14, engine speed : 1200 RPM, equivalence ratio : 0.3, and CA50=368CAD) using the skeletal mechanism and the results were compared with those of the detailed mechanism. All simulations use a single-zone homogeneous adiabatic combustion model in CHEMKIN PRO[38]. Figure 10 shows the comparison of pressure, temperature, and heat release rates (normalized by total heat release) of C_5 alcohols and PRF75 between skeletal and detailed mechanisms. The results show good agreement between skeletal and detailed mechanisms including rates of heat release, pressure, and temperature histories for a given combustion phasing (CA50=368CAD). However, intake temperatures are required to decrease by 2.4°C for 2-methylbutanol (T_{in}=85.4°C) and 3.4°C for *iso*-pentanol (T_{in}=87.1°C), and increase by 2.1°C for PRF75 (T_{in}=73.6°C) to obtain the given combustion phasing. The skeletal

mechanism successfully captures the ITHR characteristics of C_5 alcohols and LTHR of PRF75. The dominant reactions contributing to heat release at the early stage of ignition are the fuel radical reactions with molecular oxygen ($R+O_2$ reactions) and the hydrogen peroxide (H_2O_2) formation reactions according to previous analysis.

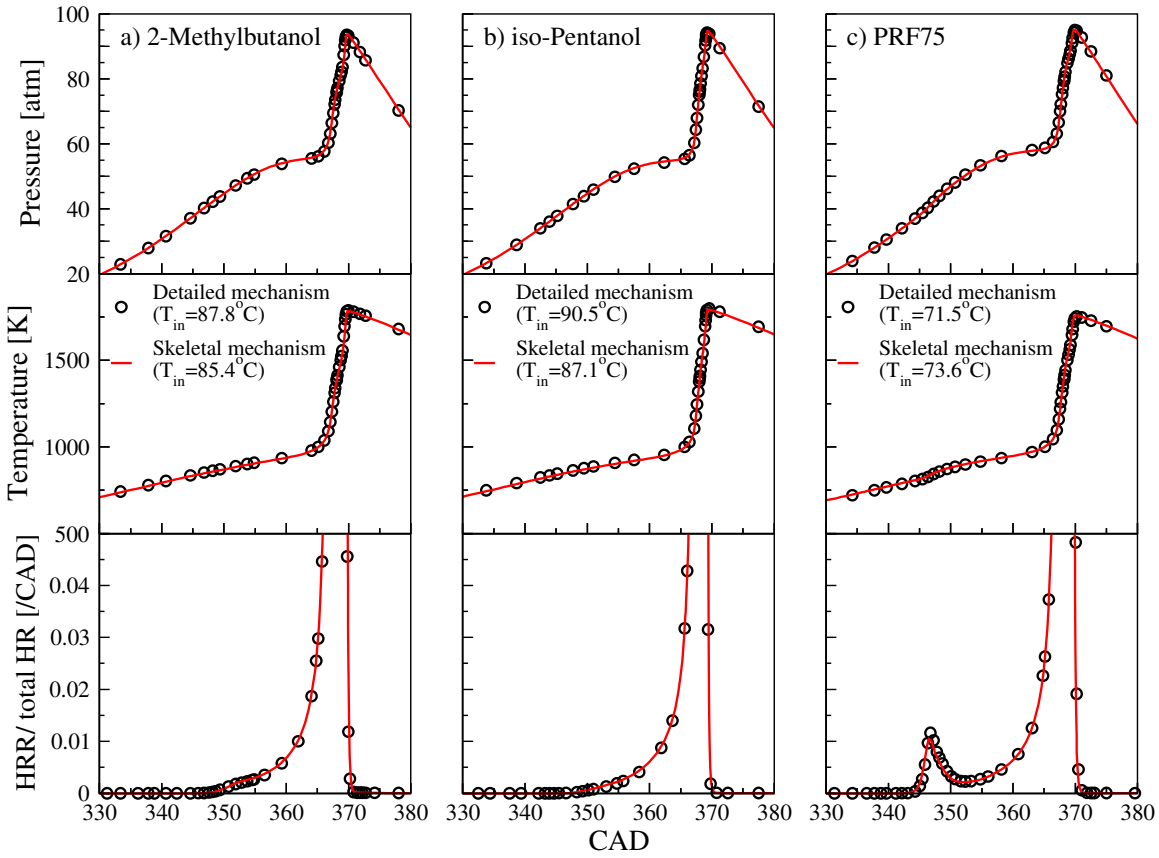

Figure 10. Comparison of detailed (symbols) and skeletal (lines) mechanisms for pressure, temperature, and heat release rate of a) 2-methylbutanol, b) iso-pentanol, and c) PRF75. (CA50≈368CAD, ϕ =0.3, P_{in}=150 kPa, and CR=14).

To examine the capability for retarding combustion phasing, the intake temperature sensitivity test was conducted using the skeletal mechanism by sweeping T_{in} from a temperature-causing advanced combustion phasing to a temperature-causing retarded combustion phasing. Figure 11A shows the comparison of sensitivities of C_5 alcohols to intake temperature.

Simulations were performed at intake pressures (P_{in}) of 150 kPa, a CR of 14, an engine speed of 1200 RPM, and an equivalence ratio of 0.3. As the intake temperature (T_{in}) decreases, combustion phasing is retarded and becomes more sensitive to changes in T_{in}. Fuels with stronger ITHRs will be less sensitive to T_{in} change for any given CA50 due to the high rate of temperature rise before hot ignition and will be less affected by random variations in combustion stability.[37] The combustion phasing of *iso*-pentanol is later than that of 2-methylbutanol at lowest intake temperature (85^{o}C) because *iso*-pentanol is less reactive at relevant constant volume ignition delay conditions (T=850K at 40atm), as shown in Figure 12. The effects of intake pressure were also investigated using the skeletal mechanism by changing P_{in}. In previous studies[51,52], gasoline has shown enhanced ITHR with boosted intake pressure, while ethanol shows no dependence on intake pressure. Figure 11B displays the comparison of intake temperatures of C_5 alcohols to maintain constant combustion phasing with various intake pressures. Simulations were performed at a CR of 14, an engine speed of 1200 RPM, and an equivalence ratio of 0.3 and varied T_{in} to maintain CA50 = 368 CAD. In this study, the P_{in} sweep was conducted at P_{in} = 110-190 kPa. Results show that the required intake temperature decreases as P_{in} increases due to the increased reactivity caused by increasing pressure. Figure 11C shows the comparison of intake temperatures at constant CA50 with various engine speeds. T_{in} were varied to maintain a constant CA50 with changing engine speed at P_{in} of 150 kPa, a CR of 14, and an equivalence ratio of 0.3. The T_{in} was increased to maintain the combustion phasing at higher engine speeds, and the simulated trend is consistent with experimental engine measurements[37].

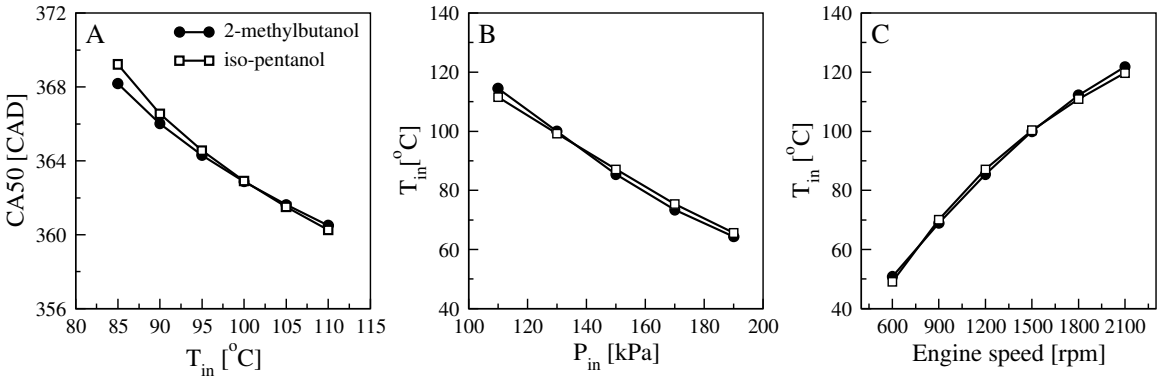

Figure 11. Sensitivity of A) intake temperature, B) pressure, and C) engine speed of C_5 alcohols. (ϕ =0.3 and CR=14).

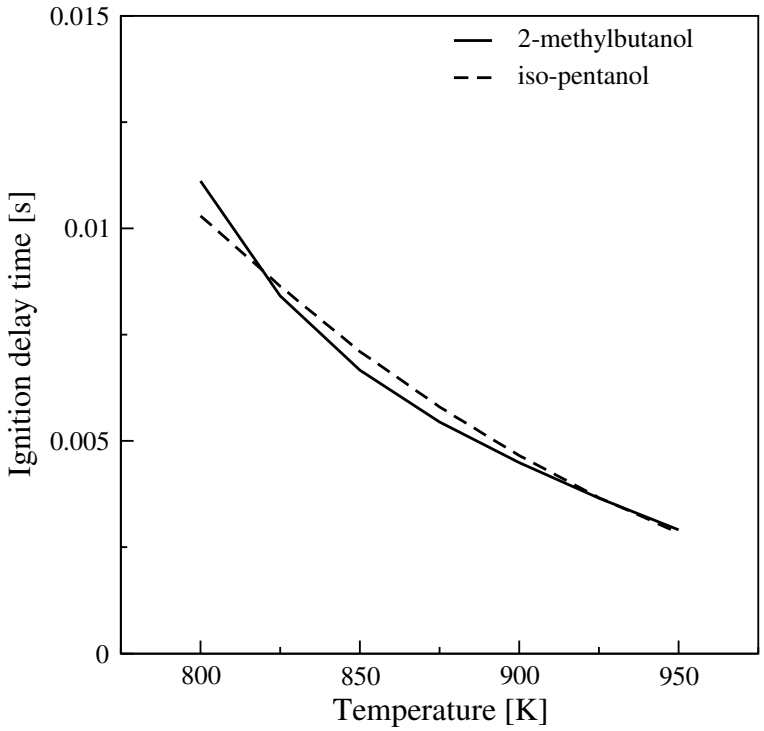

Figure 12. Ignition delay times of C_5 alcohols at relevant HCCI conditions (40 atm, ϕ =0.3).

Figure 13 shows the evolution of pressure and accumulated heat release to evaluate the effect of C_5 alcohol addition to PRF75/air mixtures in HCCI combustion. Simulations were performed at an intake pressure (P_{in}) of 150 kPa, a compression ratio (CR) of 14, an engine speed of 1200 RPM, an equivalence ratio of 0.3, and intake temperatures (T_{in}) of 90 ^{o}C using a single-

zone homogeneous adiabatic combustion model in CHEMKIN PRO[38]. As expected, combustion phasing is retarded as alcohol addition increases due to the corresponding increase in octane number, and the maximum pressure decreases as alcohol addition increases. The results also show that low-temperature heat release decreases with increasing addition of C_5 alcohols.

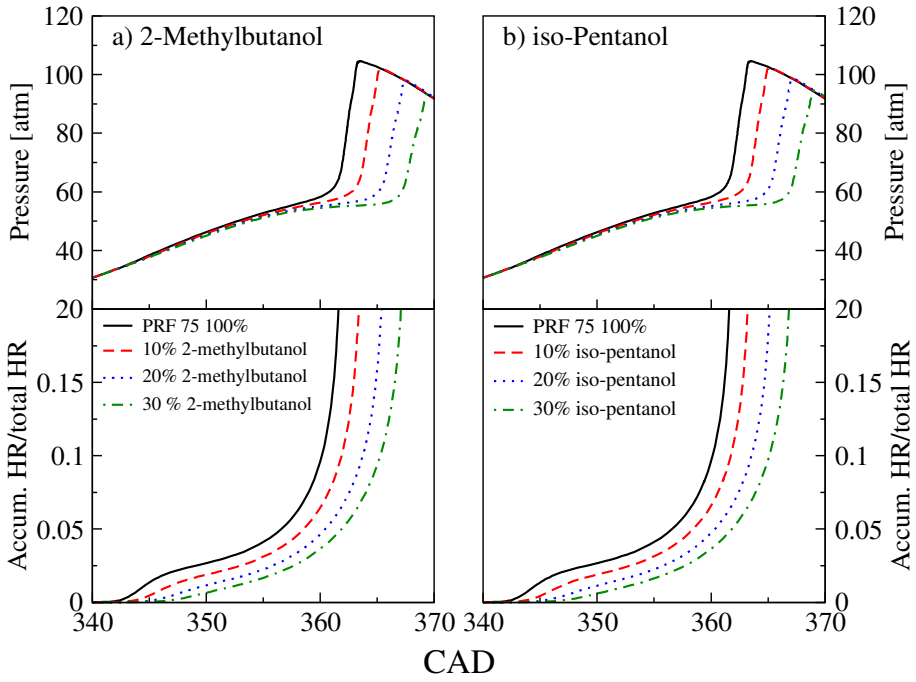

Figure 13. Comparison of pressure and accumulated heat release of PRF75 with C_5 alcohol addition. (CA50≈368CAD, ϕ =0.3, P_{in}=150 kPa, and CR=14).

To highlight the effect of alcohol addition on LTHR, heat release rates (normalized by total heat release), formaldehyde (CH_2O), and hydroperoxyl radical (HO_2) concentrations at cool flame zone are presented in Figure 14. Formaldehyde starts to accumulate during the LTHR period and present at a significant concentration during ITHR.[45] The formation of hydrogen peroxide (H_2O_2) by the recombination reactions of HO_2 radicals via $H+O_2$ reaction contributes to heat release during LTHR. The results show a significant decrease of the peak of LTHR when 30% C_5 alcohol is blended to PRF75. Figure 14 also shows the decrease in HO_2 formation during

LTHR for C_5 alcohol addition to PRF75, and these blended fuels have relatively strong ITHR characteristics.

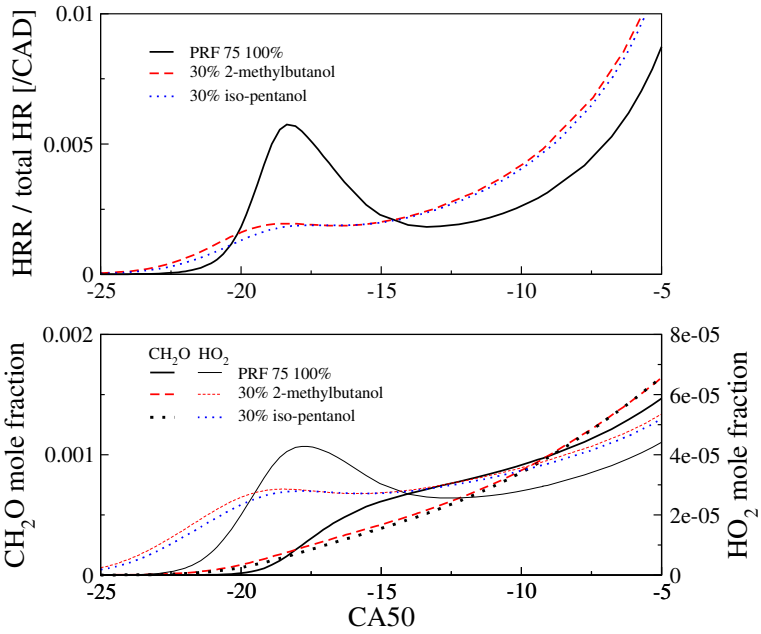

Figure 14. Comparison of heat release rate and intermediate species of PRF75 with C_5 alcohol addition at cool flame zone.

The intake temperature sensitivity test for PRF75 with C_5 alcohols was conducted to investigate the effect of alcohol addition by sweeping T_{in} from an advanced combustion phasing to a retarded combustion phasing, as shown in Figure 15. Simulations were performed at intake pressures (P_{in}) of 150 kPa, a CR of 14, an engine speed of 1200 RPM, and an equivalence ratio of 0.3. As the intake temperature (T_{in}) decreases, combustion phasing is retarded and becomes more sensitive to changes in intake temperature. Figure 15 also shows the effect of alcohol addition to delay the main combustion at lower intake temperatures. The effect of alcohol addition on combustion phasing disappears as temperature increases near 135 ^{o}C, where the reactivity of C_5 alcohols are close to those of PRFs (relevant to 950K at 40 atm). As discussed

previously, the reactivity of *iso*-pentanol is less than that of 2-methylbutanol at lowest intake temperature (75°C).

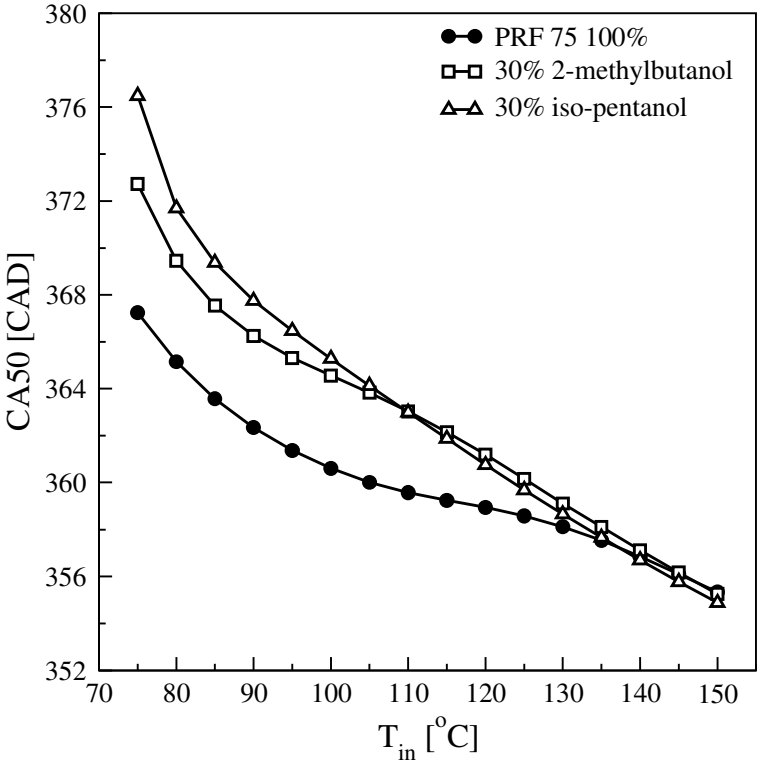

Figure 15. Comparison of intake temperature sensitivity of PRF75 with C_5 alcohol addition. (CA50≈368CAD, ϕ =0.3, P_{in}=150 kPa, and CR=14).

Conclusion

The ignition delay times of two C_5 alcohol isomers were compared with those of PRFs. Overall, ignition delay time of C_5 alcohols is slightly faster than for either PRF (heptane and iso-octane) at intermediate-temperature regions, but slower than iso-octane in the low-temperature region due to a lack of NTC behavior. The ignition delay time of 2-methylbutanol/air mixtures is similar to that of *iso*-pentanol/air mixtures at intermediate temperatures, while the ignition delay times and overall activation energy of 2-methylbutanol are lower than *iso*-pentanol at high temperatures. Reaction path analyses were conducted at intermediate- and high-temperature

conditions using a detailed chemical kinetic model to identify the important reactions controlling the ignition of both C_5 alcohol fuels.

HCCI simulations were performed to better understand the characteristics of heat release of C_5 alcohols. The detailed mechanism predicts that C_5 alcohols show relatively strong reactions at intermediate temperatures prior to hot ignition, and that both the C_5 alcohol fuels have higher HCCI reactivity than does iso-octane under the given conditions.

A new skeletal mechanism for HCCI combustion was developed using a direct relation graph with expert knowledge (DRGX) for two C_5 alcohols and PRF75. The resulting skeletal mechanism was tested against various HCCI engine combustion conditions, including intake pressure, intake temperature, and engine speed, to better understand the combustion properties of these C_5 alcohols in an HCCI engine. Combustion phasing is retarded and becomes more sensitive as intake temperature decreases and reactivity is increased with increased intake pressure. The intake temperature requirement was increased at higher engine speeds to maintain constant combustion phasing. The reactivity of *iso*-pentanol is lower than that of 2-methylbutanol in HCCI combustion under low intake temperature conditions In addition, C_5 alcohol addition to PRF75 in HCCI combustion leads to a significant decrease of LTHR and a delay the main combustion at lower intake temperatures.

AUTHOR INFORMATION

Corresponding Author

*E-mail: sungwoo.park@kaust.edu.sa

ACKNOWLEDGMENT

Research reported in this publication was supported by competitive research funding from King Abdullah University of Science and Technology (KAUST). The authors acknowledge support from the Clean Combustion Research Center under the Future Fuels research program and from Saudi Aramco under the FUELCOM program.

REFERENCES

1. Sarathy, S. M.; Oßwald, P.; Hansen, N.; Kohse-Höinghaus, K., Alcohol combustion chemistry. *Prog. Energy Combust. Sci.* **2014,** 44, 40-102.

2. Agarwal, A., Biofuels (alcohols and biodiesel) applications as fuels for internal combustion engines. *Prog. Energy Combust. Sci.* **2007**, 33, 233-271.

3. Moss, J. T.; Berkowitz, A. M.; Oehlschlaeger, M. A.; Biet, J.; Warth, V.; Glaude, P. A.; Battin-Leclerc F., An experimental and kinetic modeling study of the oxidation of the four isomers of butanol. *J. Phys. Chem. A* **2008**, 112, 10843-10855.

4. Sarathy, S. M.; Thomson, H. J.; Togbé, C.; Dagaut, P.; Halter, F.; Mounaim-Rousselle, C., An experimental and kinetic modeling study of n-butanol combustion. *Combust. Flame* **2009**, 156, 852-864.

5. Black, G.; Curran, H. J.; Pichon, S.; Simmie, J. M.; Zhukov, V., Bio-butanol: Combustion properties and detailed chemical kinetic model. *Combust. Flame* **2010**, 157, 363-373.

6. Dagaut, P.; Sarathy, S. M.; Thomson, M. J., A chemical kinetic study of n-butanol oxidation at elevated pressure in a jet stirred reactor. *Proc. Combust. Inst.* **2009**, 32, 229-237.

7. Togbé, C.; Mzé-Ahmed, A.; Dagaut, P., Kinetics of oxidation of 2-butanol and isobutanol in a jet-stirred reactor: experimental study and modeling investigation. *Energy Fuels* **2010,** 24, 5244-5256.

8. Grana, R.; Frassoldati, A.; Faravelli, T.; Niemann, U.; Ranzi, E.; Seiser, R.; Cattolica, R.; Seshadri, K., An experimental and kinetic modeling study of combustion of isomers of butanol. *Combust. Flame* **2010**, 157, 2137-2154.

9. Oβwald, P.; Güldenberg, H.; Kohse-Höinghaus, K.; Yang, B.; Yuan, T.; Qi, F., Combustion of butanol isomers – A detailed molecular beam mass spectrometry investigation of their flame chemistry. *Combust. Flame* **2011**, 158, 2-15.

10. Hansen, N.; Harper, M. R.; Green, W. H., High-temperature oxidation chemistry of n-butanol - experiments in low-pressure premixed flames and detailed kinetic modeling. *Phys. Chem. Chem. Phys.* **2011**, 13, 20262-20274.

11. Lefkowitz, J. K.; Heyne, J. S.; Won, S. H.; Dooley, S.; Kim, H. H.; Hass, F. M.; Jahangirian, S.; Dryer, F. L.; Ju, Y., A chemical kinetic study of tertiary-butanol in a flow reactor and a counterflow diffusion flame. *Combust. Flame* **2012**, 159, 968-978.

12. Sarathy, S. M.; Vranckx, S.; Yasunaga, K.; Mehl, M.; Oβwald, P.; Metcalfe, W. K.; Westbrook, C. K.; Pitz, W. J.; Kohse-Höinghaus, K.; Fernandes, R. X.; Curran, H. J., A comprehensive chemical kinetic combustion model for the four butanol isomers. *Combust. Flame* **2012**, 159, 2028-2055.

13. Frassoldati, A.; Grana, R.; Faravelli, T.; Ranzi, E.; Oßwald, P.; Kohse-Höinghaus, K., Detailed kinetic modeling of the combustion of the four butanol isomers in premixed low-pressure flames. *Combust. Flame* **2012,** 159, 2295-2311.

14. Yasunaga, K.; Mikajiri, T.; Sarathy, S. M.; Koike, T.; Gillespie, F.; Nagy, T.; Simmie, J. M.; Curran, H. J., A shock tube and chemical kinetic modeling study of the pyrolysis and oxidation of butanols. *Combust. Flame* **2012**, 159, 2009-2027.

15. Zhang, J.; Wei, L.; Man, X.; Jiang, X.; Zhang, Y.; Hu, E.; Huang, Z., Experimental and modeling study of n-butanol oxidation at high temperature. *Energy Fuels* **2012**, 26, 3368-3380.

16. Vasu, S. S.; Sarathy, S. M., On the high-temperature combustion of n-butanol: shock tube data and an improved kinetic model. *Energy Fuels* **2013**, 27, 7072-7080.

17. Cai, J.; Yuan, W.; Ye, L.; Cheng, Z.; Wang, Y.; Zhang, L.; Zhang, F.; Li, Y.; Qi, F., Experimental and kinetic modeling study of 2-butanol pyrolysis and combustion. *Combust. Flame* **2013**, 160, 1939-1957.

18. Hansen, N.; Merchant, S. S.; Harper, M. R.; Green, W. H., The predictive capability of an automatically generated combustion chemistry mechanism: Chemical structures of premixed iso-butanol flames. *Combust. Flame* **2013**, 160, 2343-2351.

19. Sarathy, S. M.; Javed, T.; Karsenty, F.; Heufer, A.; Wang, W.; Park, S.; Elwardany, A.; Farooq, A.; Westbrook, C. K.; Pitz, W. J., A comprehensive combustion chemistry study of 2,5-dimethylhexane. *Combust. Flame* **2014**, 161, 1444-1459.

20. Li, Q.; Hu, E.; Cheng, Y.; Huang, Z., Measurements of laminar flame speeds and flame instability analysis of 2-methyl-1-butanol-air mixtures. *Fuel* **2013**, 263-271.

21. Togbé, C.; Halter, F.; Foucher, F.; Mounaim-Rousselle, C.; Dagaut, P., Experimental and detailed kinetic modeling study of 1-pentanol oxidation in a JSR and combustion in a bomb. *Proc. Combust. Inst.* **2011**, 33, 367-374.

22. Zhao, L.; Ye, L.; Zhang, F.; Zhang, L. J., Thermal decomposition of 1-pentanol and its isomers: a theoretical study. *J. Phys. Chem. A* **2012**, 116, 9238-9244.

23. Heufer, K. A.; Sarathy, S. M.; Curran, H. J.; Davis, A. C.; Westbrook, C. K.; Pitz, W. J., Detailed kinetic modeling study of n-pentanol oxidation. *Energy Fuels* **2012**, 26, 6678-6685.

24. Tang, C.; Wei, L.; Man, X.; Zhang, J.; Huang, Z.; Law, C. K., High temperature ignition delay times of C_5 primary alcohols. *Combust. Flame* **2013**, 160, 520-529.

25. Li, Q.; Hu, E.; Zhang, X.; Cheng, Y.; Huang, Z., Laminar flame speeds and flame instabilities of pentanol isomer–air mixtures at elevated temperatures and pressures. *Energy Fuels* **2013**, 27, 1141-1150.

26. Dayma, G.; Togbé, C.; Dagaut, P., Experimental and detailed kinetic modeling study of isoamyl alcohol (isopentanol) oxidation in a jet-stirred reactor at elevated pressure. *Energy Fuels* **2011**, 25, 4986-4998.

27. Tsujimura, T.; Pitz, W. J.; Gillespie, F.; Curran, H. J.; Weber, B. W.; Zhang, Y.; Sung, C.-J., Development of isopentanol reaction mechanism reproducing autoignition character at high and low temperatures. *Energy Fuels* **2012**, 26, 4871-4886.

28. Welz, O.; Zádor, J.; Savee, J. D.; Ng, M. Y.; Meloni, G.; Fernandes, R. X.; Sheps, L.; Simmons, B. A.; Lee, T. S.; Osborn, D. L.; Taatjes, C. A., Low-temperature combustion chemistry of biofuels: pathways in the initial low-temperature (550 K–750 K) oxidation chemistry of isopentanol. *Phys. Chem. Chem. Phys.* **2012**, 14, 3112-3127.

29. Sarathy, S. M.; Park, S.; Weber, B. W.; Wang, W.; Veloo, P. S.; Davis, A. C.; Togbé, C.; Westbrook, C. K.; Park, O.; Dayma, G.; Luo, Z.; Oehlschlaeger, M. A.; Egolfopoulos, F. N.; Lu, T.; Pitz, W. J.; Sung, C.-J.; Dagaut, P., A comprehensive experimental and modeling study of iso-pentanol combustion. *Combust. Flame* **2013**, 160, 2712-2728.

30. Lucassen, A.; Warkentin, J.; Hansen, N.; Park, S.; Sarathy, S. M., Detailed analysis of iso-pentanol combustion chemistry in flames. The 8th US National Combustion Meeting, Park City, Utah, USA, 2013

31. Serinyel, Z.; Togbé, C.; Dayma, G.; Dagaut, P., An experimental and modeling study of 2-methyl-1-butanol oxidation in a jet-stirred reacto. *Combust. Flame* **2014**, 161, 3003–3013.

32. Zhang, X.; Yang, B.; Yuan, W.; Cheng, Z.; Zhang, L.; Li, Y.; Qi, F., Pyrolysis of 2-methyl-1-butanol at low and atmospheric pressures: Mass spectrometry and modeling studies. *Proc. Combust. Inst.* **2015**, 35, 409-417.

33. Lucassen, A,; Park, S.; Hansen, N.; Sarathy, S. M., Combustion chemistry of alcohols: Experimental and modeled structure of a premixed 2-methylbutanol flame. *Proc. Combust. Inst.* **2015**, 35, 813-820.

34. Park, S.; Mannaa, O.; Khaled, F.; Bougacha, R.; Mansour, M. S.; Farooq, A.; Chung, S. H.; Sarathy, S. M., A comprehensive experimental modeling study of 2-methylbutanol combustion. *Combust. Flame* **2015**, 162, 2166-2176.

35. Campos-Fernández, J.; Arnal, J. M.; Gómez, J.; Dorado, M. P., A comparison of performance of higher alcohols/diesel fuel blends in a diesel engine. *Appl. Energy* **2012**, 95, 267-275.

36. Gautam, M.; Martin, D. W., Combustion characteristics of higher-alcohol/gasoline blends. *Proc. IMechE. Part A: J. Power and Energy* **2000**, 214, 497-511.

37. Yang, Y.; Dec, J. E., Dronniou N, Simmons B., Characteristics of isopentanol as a fuel for HCCI engines. *SAE Int. J. Fuels Lubr.* **2010**, 3, 725-741.

38. CHEMKIN-PRO 15112. Reaction Design: San Diego, CA, 2011.

39. Metcalfe, W. K.; Burke, S. M.; Ahmed, S. S.; Curran, H. J., A Hierarchical and Comparative Kinetic Modeling Study of C_1-C_2 Hydrocarbon and Oxygenated Fuels. *Int. J. Chem. Kinet.* **2013**, 45, 638-675.

40. Mehl, M.; Pitz, W. J.; Westbrook, C. K.; Curran, H. J., Kinetic modeling of gasoline surrogate components and mixtures under engine conditions. *Proc. Combust. Inst.* **2011**, 33, 193-200.

41. Sarathy, S. M.; Kukkadapu, G.; Mehl, M.; Wang, W.; Javed, T.; Park, S.; Oehlschlaeger, M. A.; Farooq, A.; Pitz, W. J.; Sung, C.-J., Ignition of alkane-rich FACE gasoline fuels and their surrogates. *Proc. Combust. Inst.* **2015**, 35, 249-257.

42. Fieweger, K.; Blumenthal, R.; Adomeit, G., Self-ignition of S.I. engine model fuels: a shock tube investigation at high pressure. *Combust. Flame* **1997**, 109, 599-619.

43. da Silva, G.; Bozzelli, J. W.; Liang, L.; Farrell, J. T., Ethanol oxidation: Kinetics of the α-hydroxyethyl radical + O_2. J. Phys. Chem. A **2009**, 113, 8923-8933.

44. Tsujimura, T.; Pitz, W. J.; Yang, Y.; Dec, J. E., Detailed kinetic modeling of HCCI combustion with isopentanol. *SAE Int. J. Fuels Lubr.* **2011**, 4, 257-270.

45. Vuilleumier, D.; Kozarac, D.; Mehl, M.; Saxena, S.; Pitz, W. J.; Dibble, R. W.; Chen, J.-Y.; Sarathy, S. M., Intermediate temperature heat release in an HCCI engine fueled by ethanol/n-heptane mixtures: an experimental and modeling study. *Combust. Flame* **2014**, 161, 680-695.

46. Sjöberg, M.; Dec, J. E., Comparing late-cycle autoignition stability for single- and two-stage ignition fuels in HCCI engines. *Proc. Combust. Inst.* **2007**, 31, 2895-2902.

47. Liu, W.; Sivaramakrishnan, R.; Davis, M. J.; Som, S.; Longman, D. E.; Lu, T., Development of a reduced biodiesel surrogate model for compression ignition engine modeling. *Proc. Combust. Inst.* **2013**, 34, 401-409.

48. Sarathy, S. M.; Niemann, U.; Yeung, C.; Gehmlich, R.; Westbrook, C. K.; Plomer, M.; Luo, Z.; Mehl, M.; Pitz, W. J.; Seshadri, K.; Thomson, M. J.; Lu, T., A counterflow diffusion flame study of branched octane isomers. *Proc. Combust. Inst.* **2013**, 34, 1015-1023.

49. Lu, T.; Law, C. K., A direct relation graph method for mechanism reduction. *Proc. Combust. Inst.* **2005**, 30, 1333-1341.

50. Lu, T; Law, C. K., Linear time reduction of large kinetic mechanisms with directed relation graph: n-Heptane and iso-octane. *Combust. Flame*, **2006**, 144, 24-36.

51. Dec, J. E.; Yang, Y., Boosted HCCI for high power without engine knock and with ultra-low NOx emissions - using conventional gasoline. *SAE Int. J. Engines* **2010**, 3, 750-767.

52. Sjöberg, M.; Dec, J. E., Comparing late-cycle autoignition characteristics and HCCI performance for wide ranges of engine speed, load and boost. *SAE Int. J. Engines* **2010**, 3, 84-106.